5
Fluviodeltaic Reservoir, South Belridge Field, San Joaquin Valley, California

Donald D. Miller, John G. McPherson, and Thomas E. Covington

Mobil Exploration & Producing U.S., Inc., Denver, Colorado 80217; Mobil Research & Development Corporation, Dallas, Texas 75244; Mobil Exploration & Producing U.S., Inc., Denver, Colorado 80217

Introduction

A high percentage of the oil produced from sandstone reservoirs comes from fluviodeltaic sandstones. The abundance of high-quality reservoir sand, the ideal location relative to downdip source beds, and the high potential for stratigraphic trap development all make this depositional setting a favored target for explorationists. However, the sand-body architecture and reservoir quality of fluviodeltaic sandstones commonly display extreme variability over short vertical and lateral distances due to depositional controls. The fluvial-dominated delta system described in this chapter displays a wide spectrum of depositional settings from sandy braided fluvial to muddy delta front. This case study presents an opportunity to compare and contrast the reservoir characteristics of distal-bar, mouth-bar, meandering fluvial, and braided fluvial sands from the same depositional system in a single field, with well spacing close enough to make correlations relatively certain. Sand-body geometries range from sheets to shoestrings, and reservoir quality ranges from excellent to poor. The case study illustrates the importance of understanding a reservoir at all scales, from depositional setting to pore-throat geometry.

The Pleistocene Tulare Formation at South Belridge Field is a giant heavy-oil reservoir composed of unconsolidated sediments deposited in a fluviodeltaic setting. Small-scale reservoir geometries are defined and exploited by a high density of well penetrations. More than 6,000 closely spaced and shallow wells are the key to producing more than an estimated 1 billion barrels (1.6×10^8 m^3) of oil from hundreds of layered and laterally discontinuous reservoir sands. Wells are typically spaced 200 to 500 feet apart (61–152 m) for optimal heavy-oil production in steamflood patterns and drilled to a total depth of 1,000 feet (305 m) within the 14 square mile (36 km^2) producing area.

South Belridge Field's annual production ranks among the top five fields in the United States. It is one of several giant fields in the oil-rich San Joaquin Valley of California (Fig. 5-1). Although the field contains several producing formations, only the main producing reservoir, the Pleistocene Tulare Formation, is the subject of this chapter.

The discovery well was completed in 1911 at a depth of 782 feet (238 m) with initial production of 100 BOPD (16 m^3/D) (California Division of Oil and Gas, 1950). The well was located next to an outcrop of dry oil sand in a creek bed. Historically, development was slow and sporadic, as dictated by fluctuating market demand for heavy asphaltic crude oil. Fieldwide development recently intensified, concurrent with the development of in situ combustion and steamflood technology. Continued development has resulted in 6,100 active wells (Fig. 5-2) with daily production of approximately 170 MBO (2.7×10^4 m^3) (California Division of Oil and Gas, 1987) and annual production of 64 MMBO (1.0×10^7 m^3) (Oil and Gas Journal, 1988). Cumulative field production has been approximately 700 MMBO (1.1×10^8 m^3), and additional recoverable reserves are

Casebooks in Earth Science
Sandstone Petroleum Reservoirs
Eds.: Barwis/McPherson/Studlick

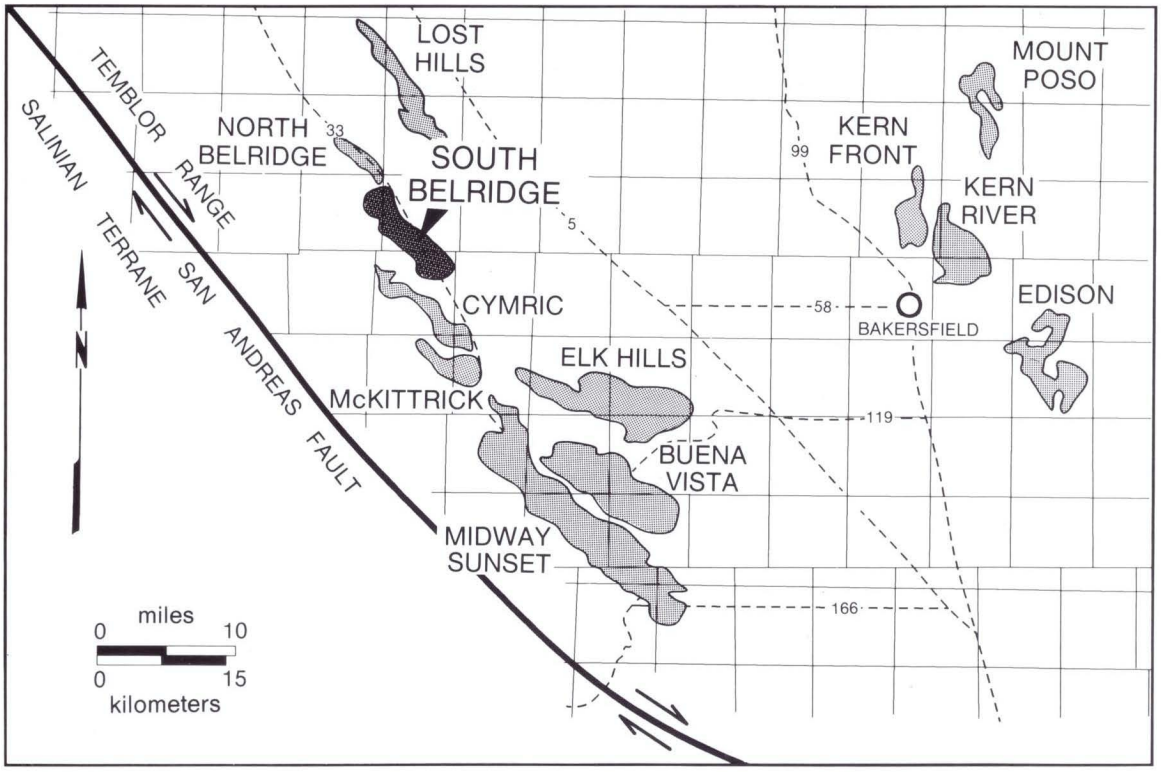

Fig. 5-1. Location map showing South Belridge Field, other giant heavy oil fields, and the San Andreas fault in the southern San Joaquin Valley, California.

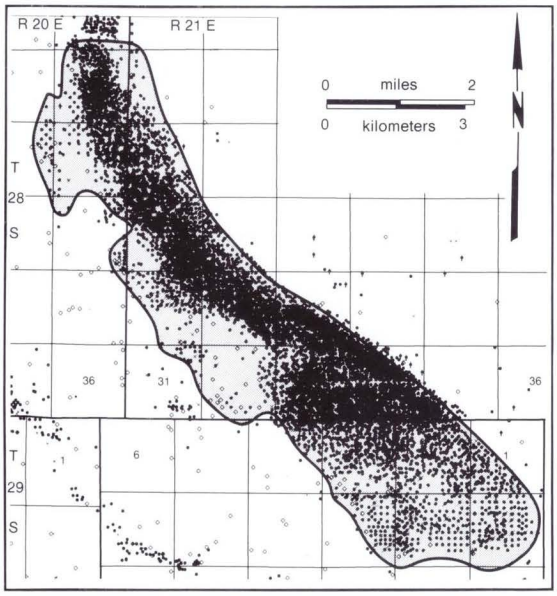

Fig. 5-2. Well location map of South Belridge Field showing locations of 6,100 active wells. (Permission to publish from Petroleum Information, 1988)

approximately 500 MMBO (8.0×10^7 m^3) (California Division of Oil and Gas, 1987).

Regional Data

Location

South Belridge Field is located on the western side of the San Joaquin Valley in Kern County, California, 100 miles (160 km) north of Los Angeles and 40 miles (64 km) west of Bakersfield (Fig. 5-1). The most prominent local geologic feature is the San Andreas fault, which is 12 miles (19 km) southwest of the field. This fault system is the western transform margin of the North American plate and has been a major influence on San Joaquin basin geologic history.

Regional and Tectonic Setting

Regional tectonism strongly controls the character of central California sedimentary basins, as forearc

basins were replaced in Tertiary time by localized borderland basins related to strike-slip faults (Graham, 1987). A number of detailed regional syntheses describe the dynamic basinal tectonic setting and the resulting framework for abrupt and complex facies changes in detail (Atwater, 1970; Nilsen and Clarke, 1975; Dickinson et al., 1979; Webb, 1981; Bartow, 1987; Namson and Davis, 1988). The elongate San Joaquin basin first developed as part of the Mesozoic Great Valley forearc basin (Ingersoll, 1979) and consisted chiefly of a marine shelf and slope largely open to the west (Clarke et al., 1975). It subsequently evolved into a late Cenozoic intermontane basin as strike-slip movement along the San Andreas fault and related tectonic events progressively closed off the basin. The change from convergent to transform margin imposed a new structural character and changed the style of sedimentation during the late Cenozoic.

Patterns of sediment accumulation in the western San Joaquin basin were directly influenced by the mountains which bordered the basin on the west (Lennon, 1976). Granitic highlands of the Salinian terrane west of the San Andreas fault and the adjacent Temblor uplift east of the San Andreas fault provided the provenance for the feldspar-rich sands of the Pleistocene Tulare Formation that constitute the Tulare reservoir at South Belridge Field. The final marine regression of the San Joaquin basin began in the late Miocene and continued through the Pliocene as progradation and aggradation of coarse clastic sediments from all sides of the basin outpaced subsidence (Lettis, 1982). This led to the final retreat of the sea near the end of the Pliocene (Bartow, 1987).

South Belridge Field lies on the crest of a large anticline along the western side of the San Joaquin basin. The anticline is one of many that are subparallel to the San Andreas fault system (Harding, 1976). Growth of the anticline before, during, and after deposition of the Tulare sands had an important influence on gross sand and reservoir distribution in the field area.

Stratigraphy

Two major Neogene erosional unconformities are present at South Belridge Field. A late Miocene unconformity is overlain by the Mio-Pliocene Etchegoin, Pliocene San Joaquin, and Pleistocene Tulare formations (Fig. 5-3). The Etchegoin Formation is predominantly marine and wedges out on the flanks

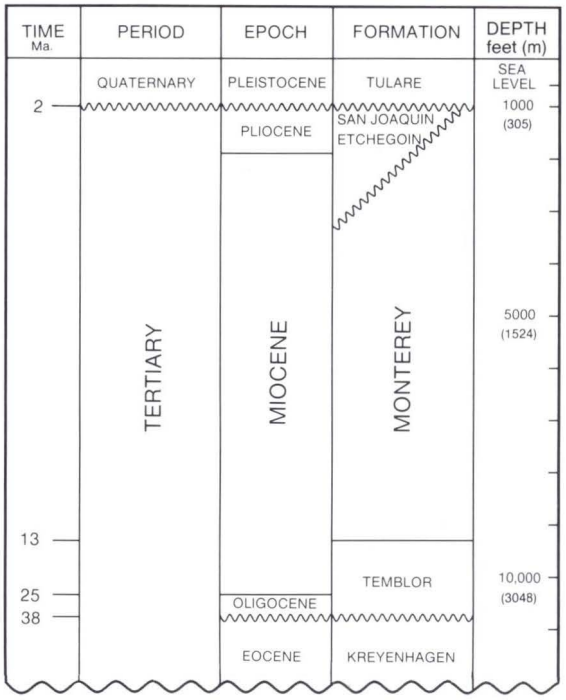

Fig. 5-3. Simplified stratigraphic section showing geologic ages and unconformable contacts between the Pleistocene Tulare Formation and the Pliocene Etchegoin and San Joaquin formations and the upper Miocene in South Belridge Field.

of the South Belridge anticline. The overlying San Joaquin Formation represents generally lacustrine and brackish-water environments (Barbat and Galloway, 1934). It also wedges out on the South Belridge anticline and overlaps onto the Miocene deposits.

The second unconformity occurs where the basal Tulare truncates the Etchegoin, San Joaquin, and Miocene Monterey formations on the South Belridge anticline. Structural deformation and erosion created a complex and irregular surface. The Tulare was then deposited unconformably on both the Pliocene and the Miocene cores of the structure, becoming conformable with upper Pliocene sediments toward the center of the basin to the east.

The Pleistocene Tulare Formation contains the youngest folded strata in the western San Joaquin basin (Fig. 5-3). This nonmarine sequence (Woodring et al., 1940; Stanton and Dodd, 1970) represents filling of the southern San Joaquin basin during Pleistocene time. Sediment was fed from nearby basin-margin highlands, via coarse-grained deltas, into the large brackish to freshwater Tulare Lake. Both fan-delta and braid-delta depositional systems

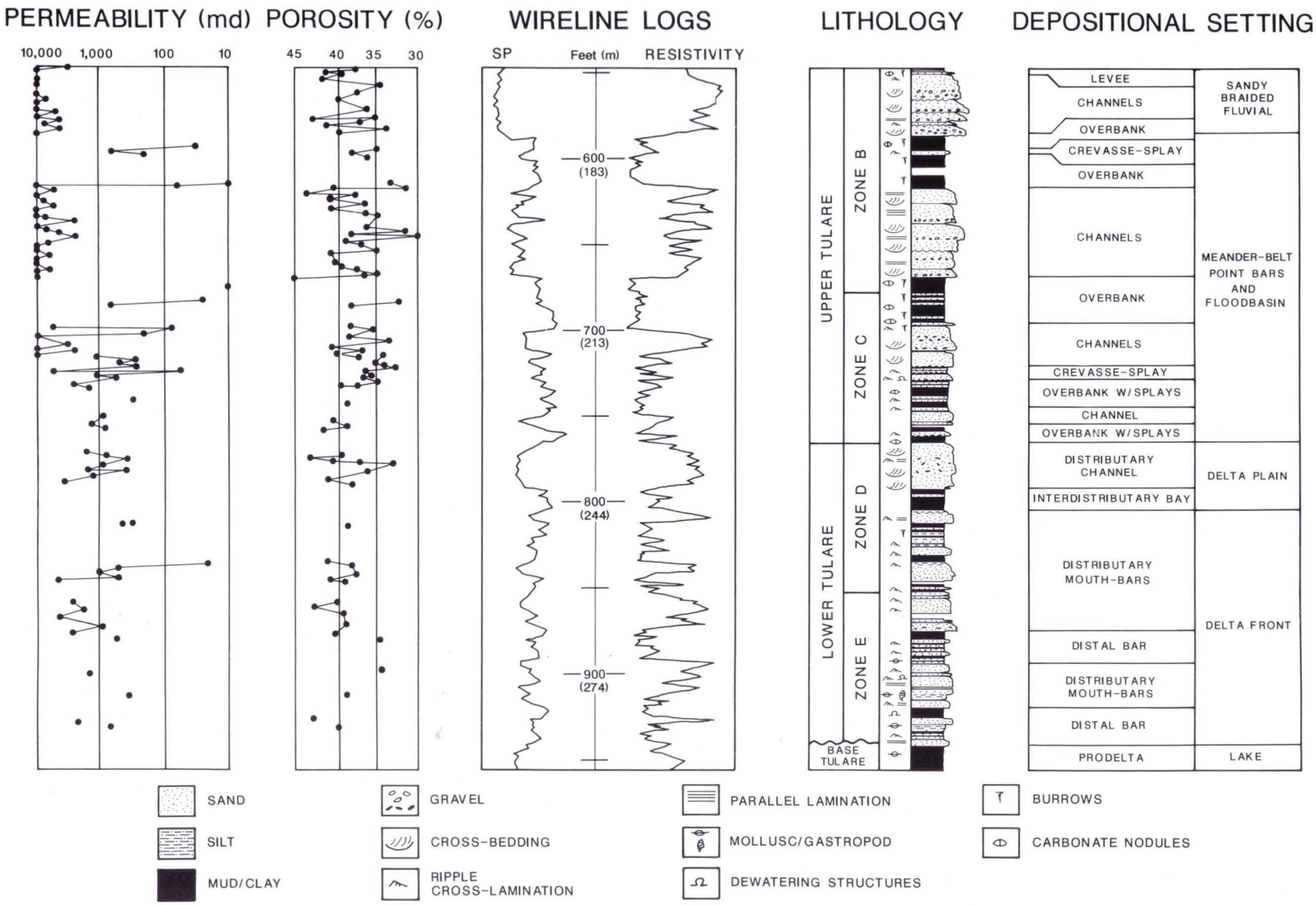

Fig. 5-4. Composite log showing reservoir zones, typical log responses, reservoir quality, and depositional lithofacies for lower Tulare deltaic sands and upper Tulare fluvial sands. The porosity values are from routine analyses at ambient conditions and permeability values (air) at 300 psi (2.1×10^3 kPa) confining pressure.

(terminology of McPherson et al., 1987) are represented in the Tulare Formation.

Tulare stratigraphy at South Belridge Field is locally subdivided into upper and lower divisions, each containing several reservoir zones (Fig. 5-4). The upper Tulare division includes zones A, B, and C. The lower Tulare division includes zones D, E, and in some places F and G. These divisions are based on general aspects of reservoir behavior and early mapping of oil-water contacts. They are not formally recognized elsewhere in the basin. This reservoir stratigraphy underlies the widespread lacustrine Tulare Corcoran Clay stratigraphic marker.

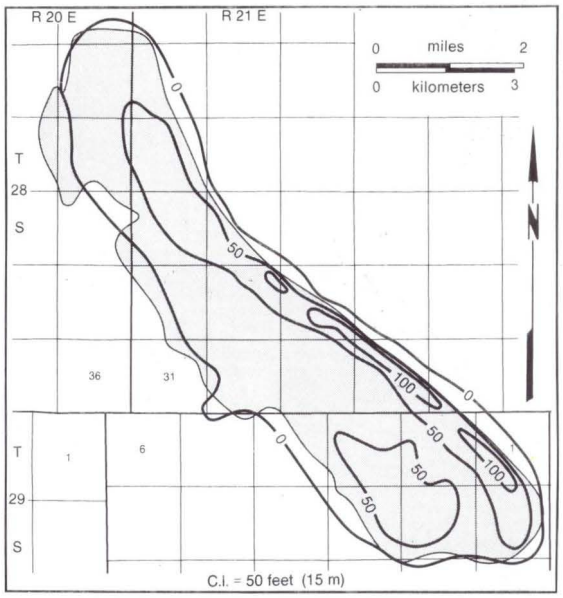

Fig. 5-5. Lower Tulare oil-sand thickness map indicating widespread distribution of sands on the flanks of the anticline in the southern part of South Belridge Field. Sands thicken basinward to the northeast and pinch out to the north and west, creating a stratigraphic trap at the northern end of the field.

Reservoir Characterization

Geometry

Reservoir geometries in the Tulare occur on two major scales and show two influences: a large-scale structural configuration, and smaller-scale depositional controls. The South Belridge structure is a large southeast-plunging anticline, but within the structure are complex, small-scale, reservoir geometries created largely by the depositional setting. The geometry of individual sand bodies and the effective reservoir geometry of interconnected sand bodies show considerable vertical and lateral variations resulting from temporal and spatial changes in the depositional setting. The upper and lower Tulare reservoir sands consequently display quite different reservoir geometries as a result of their differing depositional settings. Syndepositional growth of the South Belridge anticline further complicated the gross sand-body distributions and resulting reservoir geometries.

Geometries have been interpreted from wireline-log correlations, core facies analysis, log character, producing characteristics, steam pathways, and comparison to nearby Tulare outcrops. Preserved cores from 21 wells and information from unpreserved, disaggregated cores from 221 older wells support log correlations of 1,700 wells in the southern area of the field, the primary area of this study. Previous fieldwide studies by Mobil Oil Corporation used more than 1,000 well logs in the adjacent northern area of the field.

The lower Tulare reservoir geometries are the product of distributary-channel, distributary-mouth-bar/inner-fringe, and distal-bar/outer-fringe depositional facies (Fig. 5-4). A typical lower reservoir unit comprises a 5 to 15-foot (1.5–4.6 m) thick sand body interbedded with clays of lacustrine and interdistributary-bay origin. Moderate reworking of the delta front created a shore-parallel (SE-NW) orientation with the exception of a few distributary channel sands. The lower Tulare sands are highly stratified and are distributed throughout the producing area of the field (Fig. 5-5) and broader region (Lennon, 1976). Reservoir sands and overlying clay strata typically have very good lateral continuity, as illustrated by each of the lower sand horizons displaying separate oil-water contacts. Nonproductive sands of greater thickness occur off structure toward the basin center and link the producing reservoir with an extensive, active aquifer (Fig. 5-6). Productive reservoir sands are thicker in the southern portion of the field. The total interval thickness of the lower Tulare ranges between 100 and 300 feet (30–91 m), and oil-producing reservoir sands total as much as 150 feet (46 m) thick.

The upper Tulare sand distribution is somewhat restricted over the field as a product of its fluvial deposition (Fig. 5-7). The sands thin and pinch out in the northwestern area of the field. The thickest producing sands occur on both flanks of the anticline and thin over the crest in the southern portion of the field

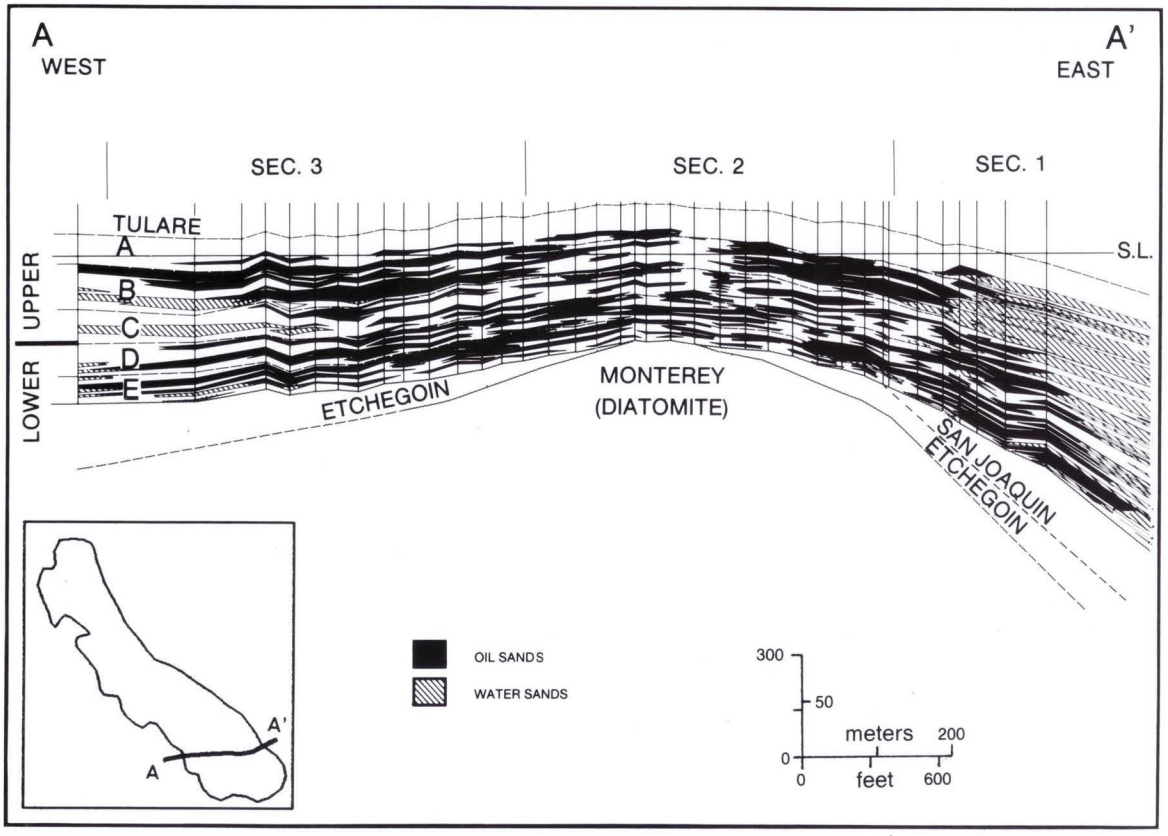

Fig. 5-6. Geologic cross section illustrating structural and stratigraphic relationships of Tulare reservoir sands. Well locations are represented by the vertical lines and the datum (S.L.) is sea level. Note the highly layered and laterally discontinuous nature of reservoirs sands, each horizon with its own oil/water contact.

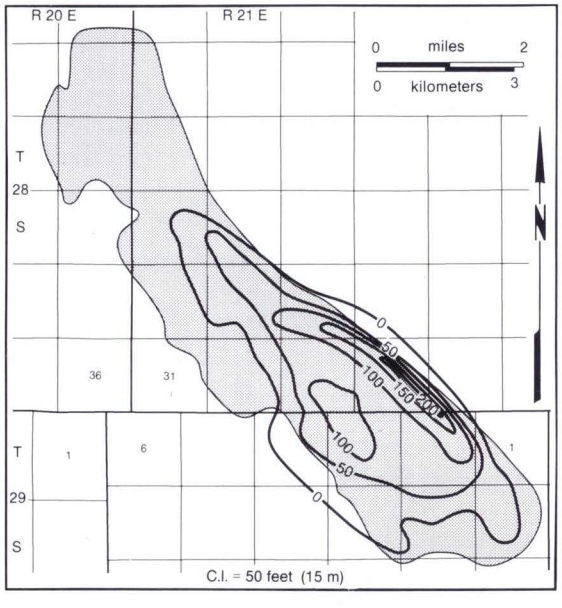

(Figs. 5-6, 5-7). This reflects a paleotopographic influence of the developing structure on gross sediment distribution. By contrast, the lower Tulare sands exhibit greater continuity over the structure (Fig. 5-6), because as deltaic sands they were probably less susceptible to paleotopographic control.

Regionally, the upper Tulare sands are thick to the south of the field and in the general direction of the sediment source. Nonproductive, water-bearing upper Tulare reservoir quality sands are thickest basinward to the east of the anticline, similar to the lower Tulare reservoir sands. West of the field these upper reservoir sands thin and pinch out. The total

Fig. 5-7. Upper Tulare oil-sand thickness map showing thickest sands on the flanks of the anticline in the southern part of South Belridge Field.

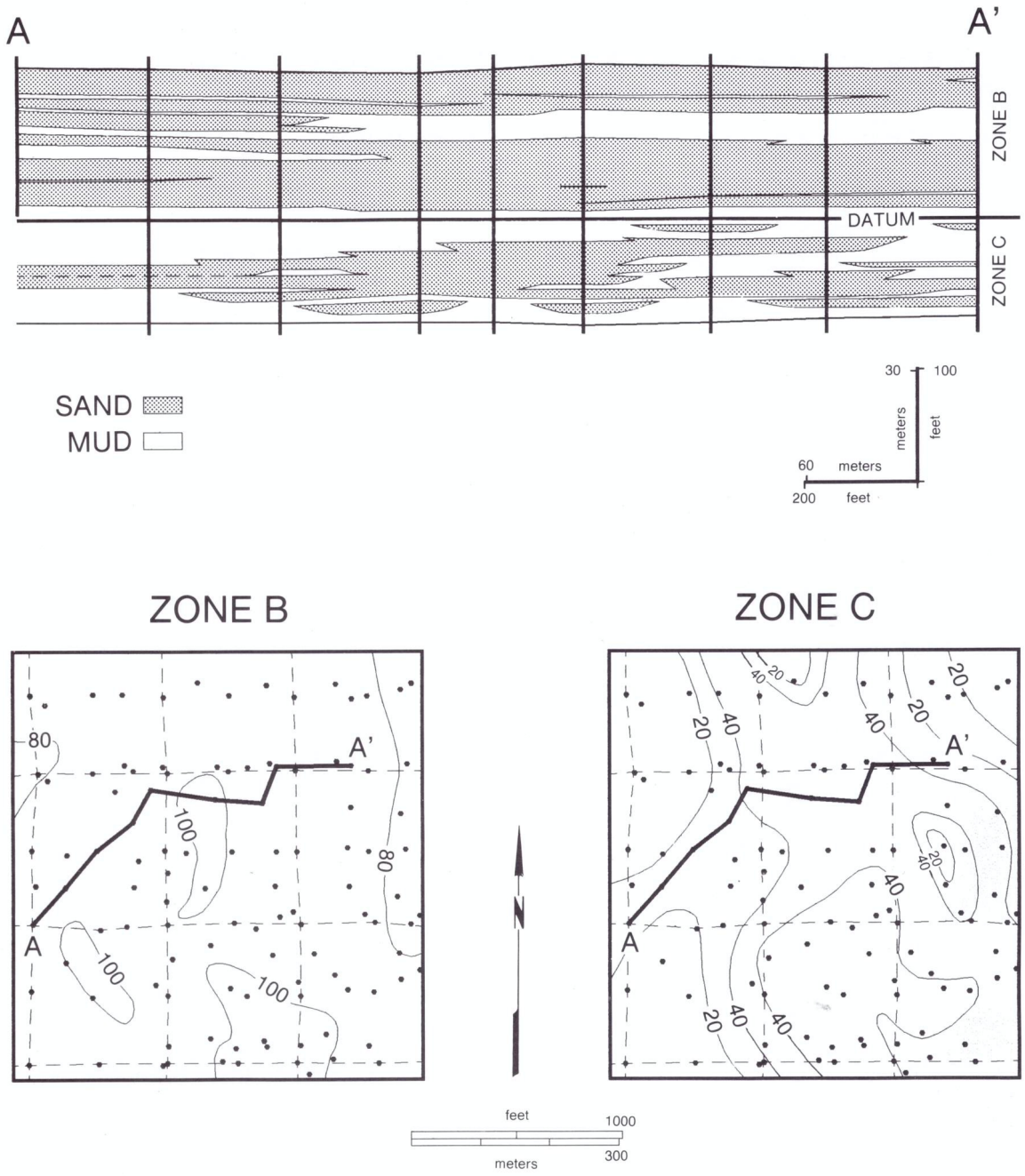

Fig. 5-8. Detailed upper Tulare stratigraphic cross section A-A′ with the corresponding net sand maps of reservoir zones B and C. Well locations on the cross section are represented by the vertical lines, and the stratigraphic datum is the contact between the two reservoir zones. The cross section illustrates the scale and variability of vertical and lateral reservoir continuity. Note the discontinuous and highly channelized character of the fine-grained meander-belt sands of zone C. By contrast, the overlying coarse-grained meander-belt sands (lower B zone) and braided fluvial sands (upper B zone) have a sheet-like character with high lateral continuity. The corresponding net sand maps clearly show these differences in sand distribution.

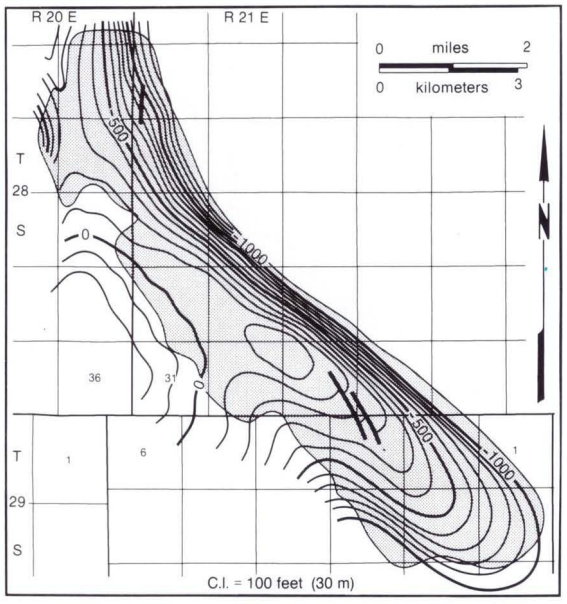

Fig. 5-9. Structural configuration of South Belridge Field reflecting the southeasterly plunging anticline in the southern area of the field and a broad saddle in the northern area of the field. (From and reprinted by permission of California Department of Oil and Gas, 1985.)

interval thickness of the upper Tulare reservoir within the producing area ranges from 300 to 450 feet (91–137 m), and the reservoir sands total as much as 230 feet (70 m) thick.

At a smaller scale, the upper Tulare reservoir geometries are the product of numerous fluvial channel sands. A reservoir unit typically consists of one or multiple stacked and amalgamated channel sands (Fig. 5-8). Reservoirs in the upper Tulare zones are commonly less continuous than for the lower Tulare zones due to the "shoestring" geometry of many individual channel sands. This is most evident in the zone A and zone C sands, which typically show less amalgamated stacking and are encased in overbank/interchannel muds. In contrast, the zone B sands show amalgamation and multilateral stacking which significantly increases the sand-body connectedness and creates a much larger effective reservoir geometry. The vertically stacked and laterally coalesced sand bodies produce a sheet-like reservoir flow unit (Fig. 5-8). Reservoir sand-body widths for the meander-belt sands in the upper Tulare zones have been calculated from paleohydrologic studies of the system (using the methodology of Ethridge and Schumm, 1978; Fielding and Crane, 1987) and average 500 feet (152 m), with a range from 150 to 1,500 feet (46–460 m). These calculated widths were confirmed by detailed sand-body mapping and coring in a selected 10-acre (4.1-ha.) pattern of the field. The sand-body widths have a direct bearing on well-spacing design.

Trapping Mechanism

Source Rock. The presumed source for the Tulare oil is the underlying Miocene Monterey Formation, which is an organic-rich unit in most areas of California. Total organic carbon (TOC) values greater than 5% (weight) are common in the San Joaquin basin and range from 0.40 to 9.16% (Graham and Williams, 1985). The heavy oil in the Tulare Formation at South Belridge is biodegraded and has characteristics of water washing as evidenced by oil fingerprint data.

Migration. The subcropping relationship of the Monterey Formation source rock to the Tulare Formation in the southern axial portion of the anticline provided the necessary pathway for hydrocarbon charge. The basal Tulare unconformity truncates Monterey rocks on the crest of the anticline, with the deeper Monterey Formation more sharply folded than the Tulare. Dips are commonly greater than 45°. Pre-Tulare and syndepositional hydrocarbon migration is suggested by tar mats in the sediments bounding the unconformity.

Seal. The Tulare hydrocarbon trap is controlled by a combination of structural and stratigraphic factors. Structurally, the overprint of the southeast-plunging Belridge anticline controls the reservoir's overall dimensions (Fig. 5-9). A basin-edge stratigraphic pinch-out provides the principal trapping mechanism in the northern portion of the field.

The greatest area of hydrocarbon entrapment occurs in the lowermost reservoir zones due to the history of continued folding and the stratigraphy of individual reservoir sand horizons encased in sealing clays and muds. The shallowest reservoir zones have minimal structural relief which results in a smaller area of hydrocarbon entrapment. The deepest horizons have the greatest structural relief and the largest area of hydrocarbon entrapment. The resulting "Christmas tree" shape of numerous stacked oil-water contacts in cross-sectional configuration is largely due to the structural arrangement (Fig 5-6).

Fluid-level traps (Foss, 1972) and tar-seal traps also provide local constraints at South Belridge Field. The fluid level, which is usually the ground-

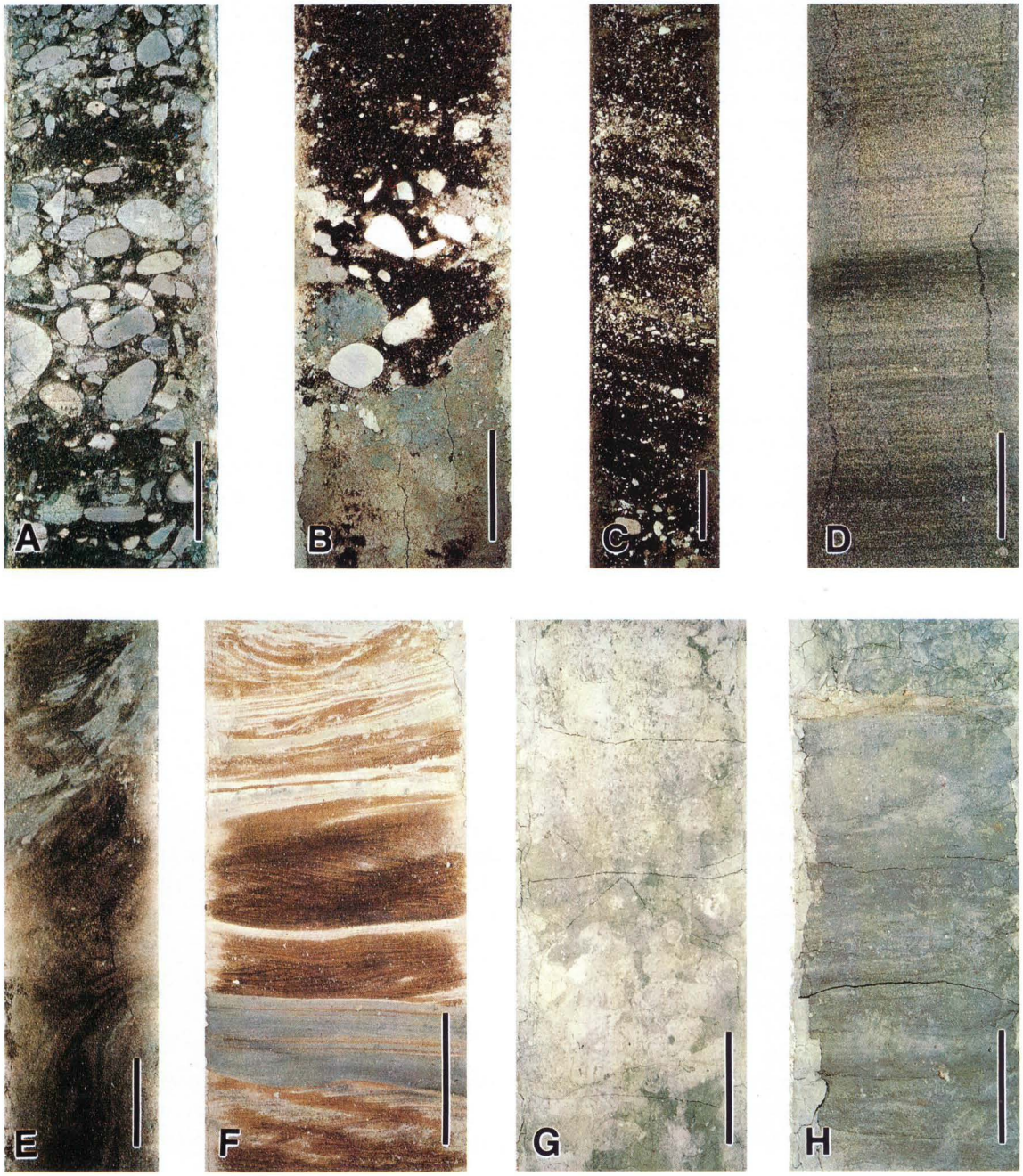

Fig. 5-10. The scale bar is 2 inches (5 cm). (A) Pebble gravel of lithofacies G. The gravel is rich in diatomaceous shale clasts and is a channel-lag deposit. (B) The basal and erosional contact of a channel sand (oil-saturated lithofacies G and S_1) and underlying overbank mud (lithofacies M). Mud intraclasts eroded from the underlying unit can be seen as a lag gravel. (C) Cross-bedded and oil-saturated gravelly (pebbles and granules) sand of lithofacies S_1. (D) Parallel-laminated fine-grained sand of lithofacies S_2. (E) Dewatering structures in fine-grained, heavy-oil-saturated sand of lithofacies S_2. (F) Ripple cross-laminated very fine-grained sand of lithofacies S_3. (G) Carbonate-cemented and burrowed silt typical of lithofacies Si. (H) A mud unit with thin, interstratified silty lenses typical of lithofacies M. The bed has been extensively bioturbated.

water table, forms a trap when the oil cannot migrate upward beyond the plane of zero hydrostatic pressure. Capillary pressure is not a significant control in the highly porous and permeable Tulare reservoirs. Fluid-level traps are reported in a limited area of the field. Local tar-seal traps have been created where oil viscosity has dramatically increased to that of an immobile tar through exposure to either water washing or biodegradation processes involving oxidation and extensive bacterial activity (Connan and Coustau, 1987).

Lithofacies

Lithofacies and lithofacies associations are the key to determining depositional environments of the Tulare sands in South Belridge Field. Furthermore, reservoir quality and producibility of the Tulare are directly tied to lithofacies variability. Six principal lithofacies are recognized: (1) sandy pebble gravel; (2) cross-bedded, gravelly sand; (3) fine-grained sand; (4) ripple-laminated, very fine-grained sand; (5) silt; and (6) mud and clay. Sandy lithofacies are the principal reservoir facies, whereas insignificant reservoir volumes are associated with the gravel and silt lithofacies.

Sandy Pebble Gravel (Lithofacies G). Gravels of pebble and granule size are clast supported, mostly with a poorly sorted sand matrix (Figs. 5-10A, 5-10B). Horizontal stratification and large-scale cross-bedding are common. The clasts comprise both intrabasinal (mud "rip-ups") and extrabasinal types. The extrabasinal clasts are rich in diatomaceous shale eroded from the underlying Miocene Monterey Formation.

Cross-Bedded Gravelly Sand (Lithofacies S_1). These sands are mostly poorly sorted, fine- to coarse-grained with a gravel component that varies in size from granules to pebbles and in concentration from low to high (Fig. 5-10C). Bed thickness ranges from an inch to several feet (centimeters to meters), and normal size grading is common. Large-scale cross-bedding is common and is delineated by granule and small pebble layers and lenses. Slumped bedding and dewatering structures are present locally.

Fine-Grained Sand (Lithofacies S_2). Lithofacies S_2 consists of moderately to poorly sorted, fine-grained sands which are commonly parallel laminated or unstratified (Fig. 5-10D). Bed thickness ranges from inches to feet (centimeters to decimeters) with some upward fining in grain size. Convolute bedding and dewatering features are evident in some of these sands (Fig. 5-10E).

Ripple-Laminated, Very Fine-Grained Sand (Lithofacies S_3). Lithofacies S_3 consists of moderately sorted, very fine-grained sands, commonly displaying ripple cross-lamination (Fig. 5-10F). Unstratified and parallel-laminated beds of this lithofacies are also common. Bed thickness ranges from inches to several feet (centimeters to meters). Thin-bedded sequences of this lithofacies are commonly interbedded with mud and clay beds. Bioturbation structures are abundant in these sands, especially where they are interbedded with muds.

Silt (Lithofacies Si). Silts cap many of the thicker sand beds in the Tulare Formation and are commonly overlain by mud beds. Bed thickness ranges from fractions of an inch to several feet (centimeters to meters). Ripple cross-lamination, bioturbation structures, and localized zones of carbonate cement are all common features of this lithofacies (Fig. 5-10G).

Mud and Clay (Lithofacies M). Greenish gray muds (including clays) occur both as thick beds separating the major sand intervals, by several tens of feet (meters), and as thin beds, a few inches (centimeters) thick, within sand units. The muds are of two types, unstratified and thinly laminated. Lenticular beds of very fine-grained sand and silt are common in some mud units (Fig. 5-10H). Bioturbation structures are very common, and the degree of bioturbation varies from slight to complete. Localized zones of carbonate cement, up to 1 foot thick (30 cm), are common in many of the thicker mud units.

Depositional Setting

Specific depositional subenvironments of a fluviodeltaic setting in the Tulare Formation are interpreted on the basis of distinctive and repeated lithofacies associations. These subenvironments include (1) channel and bar, (2) levee and crevasse splay, (3) overbank/interchannel, (4) distributary-channel-mouth bar, (5) distal bar, and (6) prodelta/lacustrine basin (Table 5-1).

Channel and Bar Deposits. The upper Tulare reservoir in the southern portion of the field consists of channel and bar sands mostly of point-bar origin. They occur in units of stacked and amalgamated beds (Fig. 5-4), with individual depositional sequences that average 10 feet (3.1 m) thick and range from 5 to

Table 5-1. Lithofacies associations and their interpretations for the Tulare Formation in South Belridge Field.

Lithofacies	Lithofacies associations and depositional settings					
	Channel/bar	Levee	Overbank	Mouth bar	Distal bar	Lake
Sandy pebble gravel (G)	○					
Cross-bedded gravelly sand (S_1)	●					
Fine-grained sand (S_2)	●	○		○		
Ripple-laminated vf sand (S_3)	○	●	○	●	○	
Silt (Si)		○	○		○	○
Mud and clay (M)		○	●	○	●	●

● dominant lithofacies
○ associated lithofacies

25 feet (1.5–7.6 m). The depositional sequences typically fine upward and have a lower erosional surface overlain by a lag gravel (G) (Fig. 5-10B). They comprise cross-bedded, gravelly (pebbles and granules), fine- to medium-grained, poorly sorted sands (S_1 and S_2) at the base, with ripple cross-laminated, very fine-grained sands (S_3) at the top (Table 5-1). Levee and crevasse-splay deposits commonly directly overlie the point-bar sands.

Some channel and bar sands of the uppermost B zone are coarser grained and gravelly (pebbles and granules), more thinly bedded, and lack the well-developed upward fining cycles characteristic of the point bars of the underlying Tulare. These sequences are interpreted as braided fluvial deposits. Prominent erosional surfaces overlain by thin gravel beds delineate the base of each sequence. Large-scale cross-bedding and parallel lamination are common throughout most sequences. The high-angle cross-beds and relatively well-sorted texture suggest deposition in a downstream braided segment dominated by transverse bars.

Levee and Crevasse-Splay Deposits. Levee deposits are mostly interbedded sequences of very fine-grained sand (S_3) or silt (Si) and mud (M) (Table 5-1). Thickness varies from 2 to 10 feet (0.6–3.1 m). The sands are typically ripple cross-laminated, commonly with climbing ripples indicative of high aggradation rates. Both sands and muds are extensively bioturbated. Crevasse-splay sands are present as isolated beds of very fine- to fine-grained sand, usually ripple cross-laminated and bioturbated. Most splay sands are encased in overbank/interchannel mud and the lower contact is commonly erosional. Upper contacts are sometimes carbonate cemented and are interpreted as paleosol horizons.

Overbank/Interchannel Deposits. Overbank and interchannel deposits are a major component of the Tulare Formation in the southern portions of the field. The deposits comprise thin (less than 1 foot (30 cm) muds and clays (M) and minor silts (Si) (Table 5-1). Wavy- and lenticular-bedded sands are present locally. These overbank deposits were emplaced by interchannel sedimentation from flood-stage channel overtopping and by channel crevassing. A high degree of bioturbation in many of the interchannel sequences points to a lower delta-plain lacustrine influence. Similar to the levee and crevasse-splay deposits, carbonate-cemented paleosol horizons indicate periods of nondeposition and soil weathering.

Distributary-Channel-Mouth-Bar Deposits. The distributary mouth-bar/deltaic inner-fringe sands are moderately well sorted and very fine- to fine-grained (S_2 and S_3 (Table 5-1). These deposits have sharp but nonerosive upper and lower contacts with mud beds of lithofacies M. Prominent sedimentary structures include ripple cross-lamination, wavy lamination, and parallel lamination, but unbedded units are also common. The sedimentary structures indicate reworking of these sands by wave and current action into more areal extensive fringe sands. Although the lacustrine energy was relatively low, the episodic nature of river mouth-bar deposition allowed time for the reworking. Mouth-bar sands that are sandwiched between distal-bar and prodelta sequences indicate lateral shifting of the distributary channel in the lower delta plain.

Distal-Bar Deposits. The distal-bar/deltaic outer-fringe deposits are composed of thin bedded, ripple-laminated sand (S_3) interbedded with laminated silt (Si) and mud (M) interbeds (Table 5-1). The sand content varies from less than 5 to 30%. Bioturbated beds are common. Distal-bar deposits are most abundant in the lower Tulare (zones D and E) associated with distributary-mouth-bar sediments.

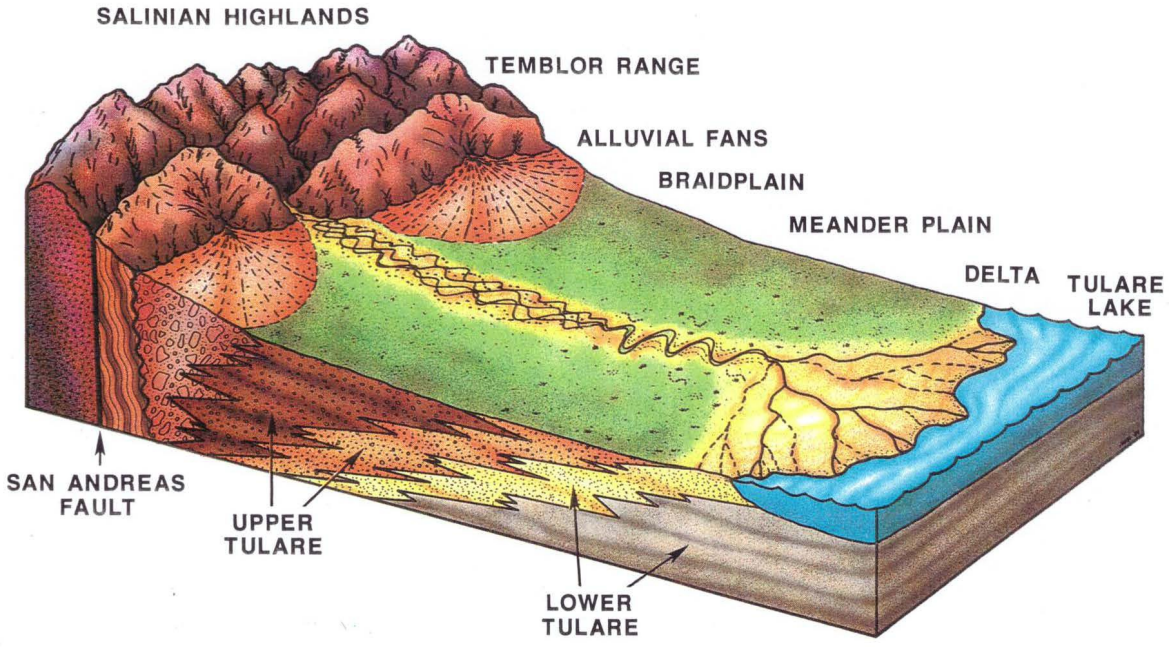

Fig. 5-11. Schematic representation of the depositional setting of the Tulare Formation at South Belridge Field.

Prodelta/Lacustrine Basin Deposits. The prodelta-lacustrine basin deposits are composed primarily of thick muds, silty muds, and clays (M) (Table 5-1). Very thin, lenticular beds of sandy silts in these deposits represent distal, delta-toe turbidite flows.

In summary, the overall depositional setting of the Tulare at South Belridge is that of a prograding fluviodeltaic system (Fig. 5-11). The lower Tulare reservoir sands (zones D and E) are mainly of delta-front and delta-plain origin, with distal-bar, distributary-mouth-bar, and a few distributary-channel sands (Fig. 5-4). The upper Tulare reservoir sands display a variety of fluvial styles. Somewhat more isolated (multistoried) fine-grained meander-belt sands (zone C) are overlain by more amalgamated (multilateral) coarse-grained meander-belt sands (lower zone B), in turn overlain by even less confined and braided fluvial sands (upper zone B). Laterally accreted point-bar deposits are common, with well-defined upward-fining sequences and associated levees and crevasse-splays. Zone A sands at the top of the reservoir sequence, although of lesser reservoir importance, establish a return to a fine-grained meander-belt system. Paleotopography created by the growing South Belridge anticline directly influenced the gross distribution of the fluvial system but had much less influence on the deltaic sands.

Petrography

The reservoir sands of the upper and lower Tulare zones are texturally and mineralogically immature (Fig. 5-12). The sands are mostly lithic feldsarenites (classification after Folk et al., 1970) comprising subequal amounts of feldspar and quartz (35–45%) and lesser amounts of rock fragments, mica, pyrite, carbonate, amorphous material, and clay minerals. Diatomaceous gravel and sand are particularly abundant in the fluvial channel sequences of the upper Tulare zones. The sands are unconsolidated and essentially "oil-cemented," although grain supported.

The clay mineral content in the reservoir facies is typically 5% and ranges from 1 to 8%. Clay minerals consist primarily of illite (60%) and smectite (40%), usually in mixed-layer morphology. These clays are only a part of the total formation fines in the reservoir which affect reservoir permeability. The total sediment fines (less than 44 microns) constitute 5 to 18% of the reservoir facies. In addition to clay minerals, they consist of clays and micas, clay- and silt-sized particles of quartz, feldspar, pyrite, calcite, and rock fragments (Fig. 5-12). Related production effects include migration of fines which plug pores and mineral dissolution and authigenesis in steam injection conditions. Higher plagioclase-to-quartz

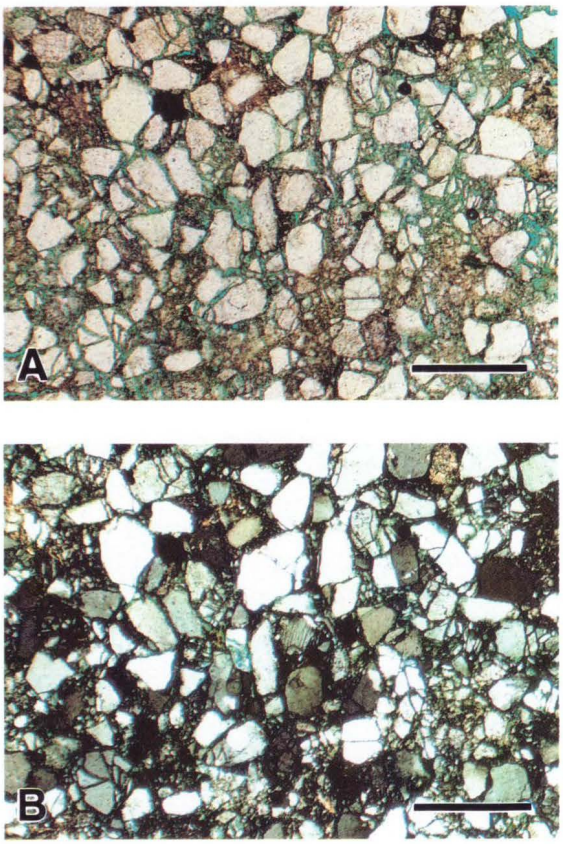

Fig. 5-12. A (plane polarized light) and B (cross polarizers): Photomicrographs of a poorly sorted, fine- to medium-grained lithic feldsarenite representative of lithofacies S_2. The sand is both texturally and compositionally immature and in places contains a matrix of silt-sized quartz and feldspar and minor (5%) clay. Porosity (blue areas in A) is mostly intergranular and well connected, but the matrix has abundant micropores that contribute to ineffective porosity. Scale bar is 0.50 mm.

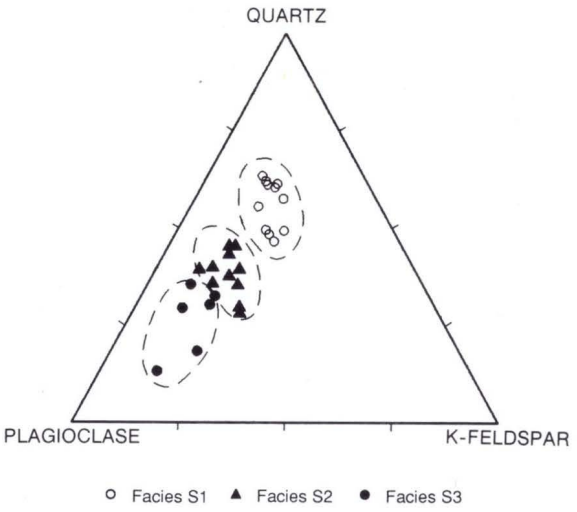

Fig. 5-13. Quartz, plagioclase, and potassium feldspar reservoir sand compositions plotted by lithofacies. S_1 is cross-bedded gravelly sand; S_2 is fine-grained sand; and S_3 is ripple-laminated, very fine-grained sand.

ratios in the finer-grained lithofacies (S_2 and S_3, as compared to S_1) are a product of composition and size sorting (Fig. 5-13); feldspar is generally more abundant in the finer-grained lithofacies.

The reservoir sands display a wide range in grain size, sorting, and shape as a product of differing depositional processes and settings of the Tulare. Grain size, the most important textural element for reservoir considerations, ranges from gravel to very fine-grained sand (Fig. 5-14). Sorting ranges from moderate to poor. The poorest sorting is found in the coarser-grained, fluvial channel sands (lithofacies S_1), whereas the best sorting is found in the delta mouth-bar sands (lithofacies S_2 and S_3). In the Tulare reservoir sands, sorting has much less influence on permeability, and therefore on oil saturation, than does grain size.

Diagenesis

The reservoir sands show almost no diagenetic modification due to their young age and very shallow burial. Compaction has been minimal because the maximum burial depths are generally less than 1,000 feet (305 m). The sands are uncemented, as are the silts and muds, with the exception of local zones of penecontemporaneous nodular carbonate.

Mineralogical changes associated with steam-rock reactions can lead to significant changes in porosity and permeability (cf. Sedimentology Research Group, 1981). Smectite-to-illite ratios in the Tulare reservoir sands show significant changes caused by thermal diagenesis resulting from steam injection. These changes result from chemical reactions involving quartz, carbon dioxide, and water:

$$\text{illite} + \text{calcite} + \text{quartz} \rightarrow \text{smectite} + \text{carbon dioxide} + \text{water}$$

Although the Tulare reservoir sands show an increased smectite-to-illite clay ratio in the steamed intervals, they do not exhibit significant reductions in porosity and permeability because of their overall low clay content. However, an increase in the smectite-to-illite ratio in the mud lithofacies greatly

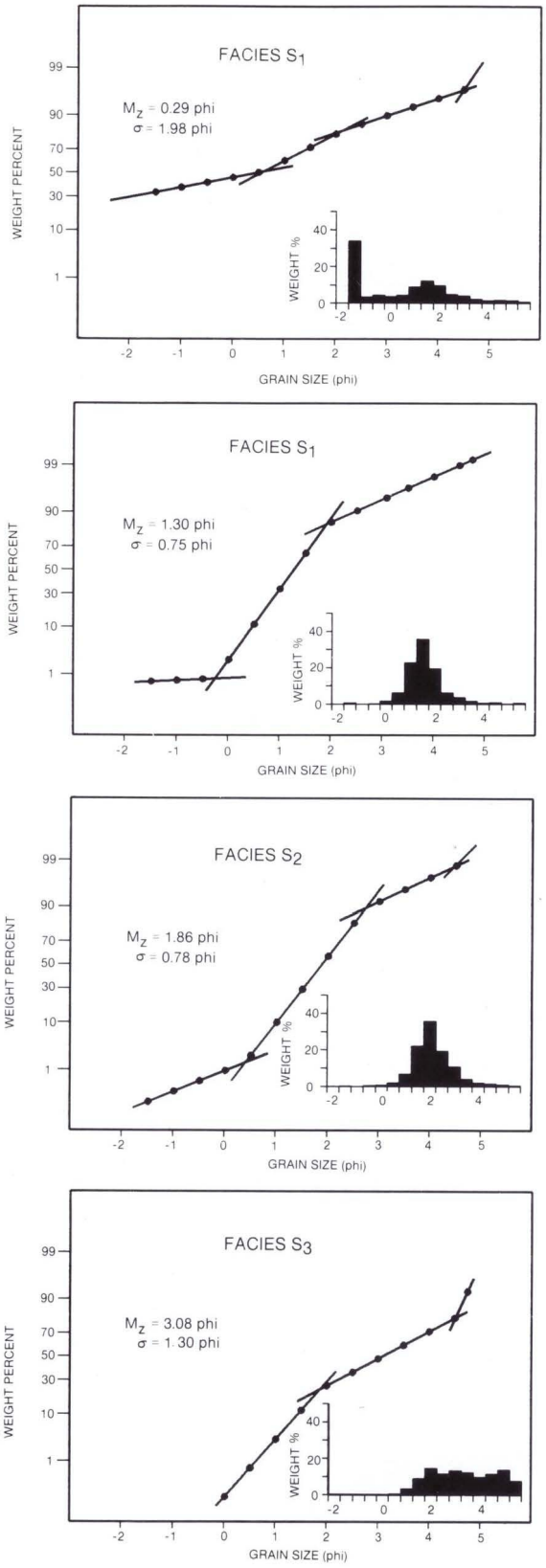

increases its effectiveness as a permeability barrier. In addition, the steam commonly precipitates secondary carbonate in the mud lithofacies. The combined effects of carbonate cementation and smectite growth create low-permeability zones or discontinuous baffles and impermeable barriers to fluid flow in the reservoir. These dynamic processes during production alter the geometry of the injected steam profile. This can occur even within thin (0.5 ft, 15 cm) mud units, as evident in cores of steamed reservoirs.

Petrophysics

Reservoir quality in the Tulare Formation is primarily controlled by lithofacies, which are the product of the depositional environment. This depositional lithofacies control of reservoir quality is clearly observed in the Tulare because of the absence of diagenesis, which overprints and complicates the depositional influences in most other sandstone reservoirs. The reservoir sands exhibit excellent reservoir quality, with an average effective porosity of 35% and 3,000 md permeability (Table 5-2) (Gates and Brewer, 1975).

Porosity, permeability, and fluid saturation measurements from routine core analysis and wireline logs have unique problems in the unconsolidated, heavy-oil sands of the Tulare Formation. Grain rearrangement during coring, wellsite, and laboratory procedures can alter significantly the physical properties of core samples (Elkins, 1972). Therefore, a correction factor is applied to ambient core porosity data in order to better calculate porosities at reservoir conditions. Core samples analyzed at ambient conditions average 2 to 3 porosity units (% absolute) greater than that measured at overburden pressure conditions. Permeability values of brine-saturated samples measured at reservoir stress conditions are approximately half of the routine permeability values measured in air. Permeability data from cores are also sensitive to alteration of the deli-

Fig. 5-14. Representative grain-size distributions of the reservoir sands plotted by lithofacies. Note that the uppermost lithofacies S_1 sample is from the base of a fluvial channel sequence and incorporates the channel-lag deposits. S_1 is cross-bedded gravelly sand; S_2 is fine-grained sand; and S_3 is ripple-laminated, very fine-grained sand.

Table 5-2. Typical values for grain size, porosity, permeability, and oil saturation for the principal lithofacies of the Tulare Formation.

Lithofacies	Mean grain size (Mz in phi)	Porosity* (ϕ)	Permeability** (md)		Oil saturation (So)
			(k_h)	(k_v)	
Sandy pebble gravel (G)	−2.5	34%	10,000	7,000	50%
Cross-bedded gravelly sand (S_1)	1.1	34%	10,000	8,000	85%
Fine-grained sand (S_2)	2.3	35%	6,000	5,000	75%
Ripple-laminated vf sand (S_3)	3.3	36%	700	300	60%
Silt (Si)	4.5	35%	50	10	15%
Mud and clay (M)	9.0	35%	0.1	0.1	0%

* Effective porosities corrected to reservoir conditions.
** Air permeabilities determined at 300 psi (2.1×10^3 kPa).

cate clay fabric caused by fluid extraction and sample drying. Oil saturations from cores are relatively accurate in these heavy-oil sands (once corrected for reservoir porosities) because of reduced flushing during drilling and coring and use of large-diameter (5 in. (13 cm)) core barrels.

Total porosity in the Tulare ranges from 32 to 42% and correlates poorly with permeability and lithofacies type (Table 5-2; Fig. 5-15). However, porosity is not a limiting factor in this reservoir. Ineffective porosity, up to 5% (absolute), is attributed to the clays and diatomaceous fragments in the finer-grained lithofacies. The diatomaceous fragments have been eroded from underlying Miocene Monterey strata.

Measured core permeability values (air at 300 psi (2.1×10^3 kPa) confining pressure) range from less than 100 to 10,000 md. These permeabilities display a strong correlation with lithofacies (Fig. 5-15). This is primarily a function of grain size variability in the lithofacies; the coarser-grained lithofacies have the highest permeabilities (Table 5-2; Figs. 5-4, 5-16) (cf. Beard and Weyl, 1973).

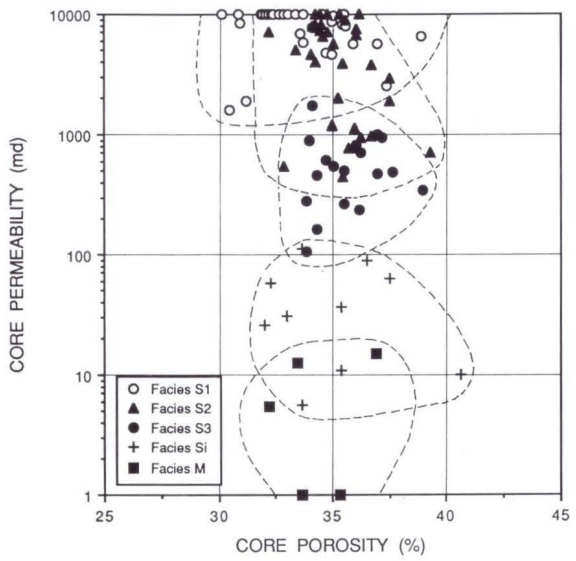

Fig. 5-15. Core porosity and permeability plotted by lithofacies. The porosities of the silt and mud lithofacies are low relative those of the sand lithofacies because of differences in compressibility. The porosity data have been corrected to reservoir conditions. Air permeability data were determined at 300 psi (2.1×10^3 kPa). S_1 is cross-bedded gravelly sand; S_2 is fine-grained sand; S_3 is ripple-laminated, very fine-grained sand; Si is silt; and M is mud.

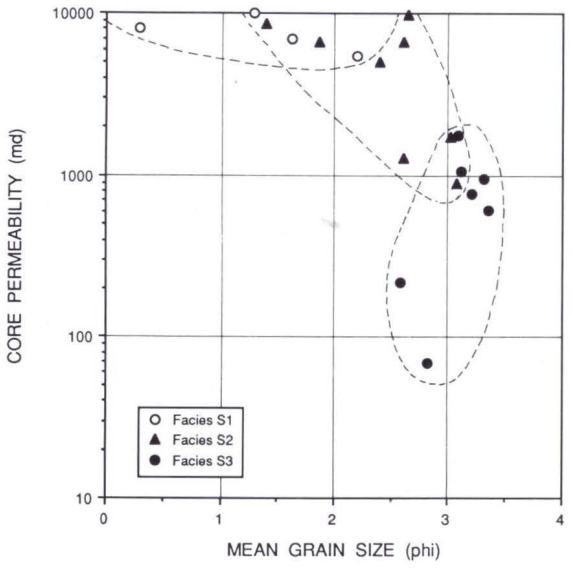

Fig. 5-16. Core permeability and mean grain size plotted by lithofacies. Permeability (air) is determined at 300 psi (2.1×10^3 kPa) confining pressure. S_1 is cross-bedded gravelly sand; S_2 is fine-grained sand; and S_3 is ripple-laminated, very fine-grained sand.

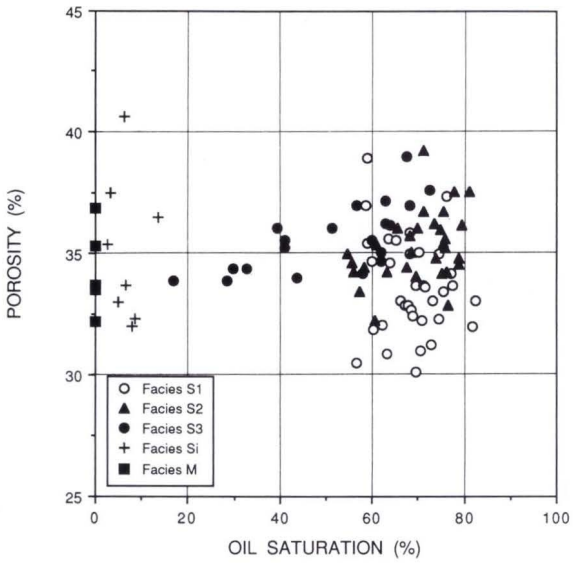

Fig. 5-17. Core porosity and oil saturation plotted by lithofacies. Porosities have been corrected for reservoir conditions. S_1 is cross-bedded gravelly sand; S_2 is fine-grained sand; S_3 is ripple-laminated, very fine-grained sand; Si is silt; and M is mud.

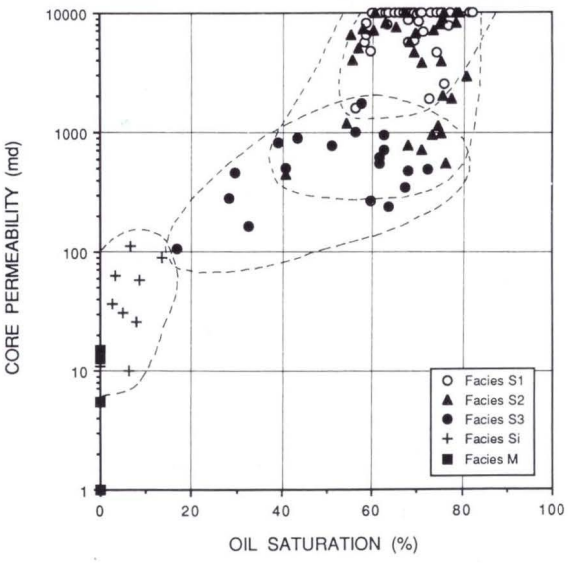

Fig. 5-18. Core permeability and oil saturation plotted by lithofacies. Permeability (air) is determined at 300 psi (2.1×10^3 kPa) confining pressure. S_1 is cross-bedded gravelly sand; S_2 is fine-grained sand; S_3 is ripple-laminated, very fine-grained sand; Si is silt; and M is mud.

Original oil saturations are assumed to have averaged 76% in the Tulare reservoir (Gates and Brewer, 1975). Oil saturations range from a maximum of 85% in sands to less than 10% in silts. The saturations of the reservoir sands are unrelated to porosity (Fig. 5-17) but are strongly correlated to permeability, grain size, and lithofacies (Fig. 5-18; Table 5-2). Lower permeability sands have greater specific surface areas and higher irreducible water saturations; the higher oil saturations correspond to the more permeable lithofacies. Vertical and horizontal distribution of these lithofacies thus controls overall oil storage capacity and producibility of the reservoir.

Wireline-log analysis has its own set of problems in these unconsolidated heavy-oil sand reservoirs. Borehole washouts from drilling are common in these unconsolidated sediments, limiting the usefulness of some logs. In addition, resistivity logs, used to calculate oil saturations, are very sensitive to variations in formation water salinity induced by the close proximity to meteoric groundwater. This is indicated by decreasing baseline resistivities in clays, which can be used to calibrate and improve log calculations. On the positive side, porosity calculated from logs has an inherent accuracy advantage of in situ measurement, avoiding the grain rearrangement problem incurred during core acquisition.

Steam injection complicates wireline surveys because the multiphase porosity system contains formation water, oil, steam, and fresh water from condensed steam. Steamed reservoir horizons produce a suppressed or inverted SP log response, a heat-induced resistivity suppression, and a "gas effect" signature on neutron-density logs (Fig. 5-19). The steamed Tulare reservoirs also have a high gamma-ray signature due to mobilized uranium roll-front concentrates carried along with the steam front.

Heterogeneities

The Tulare is a highly layered and laterally discontinuous reservoir at South Belridge Field (Figs. 5-6, 5-8). Heterogeneities in the reservoir sands control the vertical and lateral continuity on several scales. The scale of reservoir heterogeneities, relative to well spacing, determines the control on reservoir flow characteristics. The variable reservoir layering is a product of the depositional stacking of sands and muds typically creating 1 to 4 separate layers in each of the 5 reservoir zones. Lateral flow restrictions are a function of the three-dimensional sand-body geometries. The overall reservoir sequence contains laterally continuous reservoir sands in the lower zones and both coalescing and isolated "shoestring"

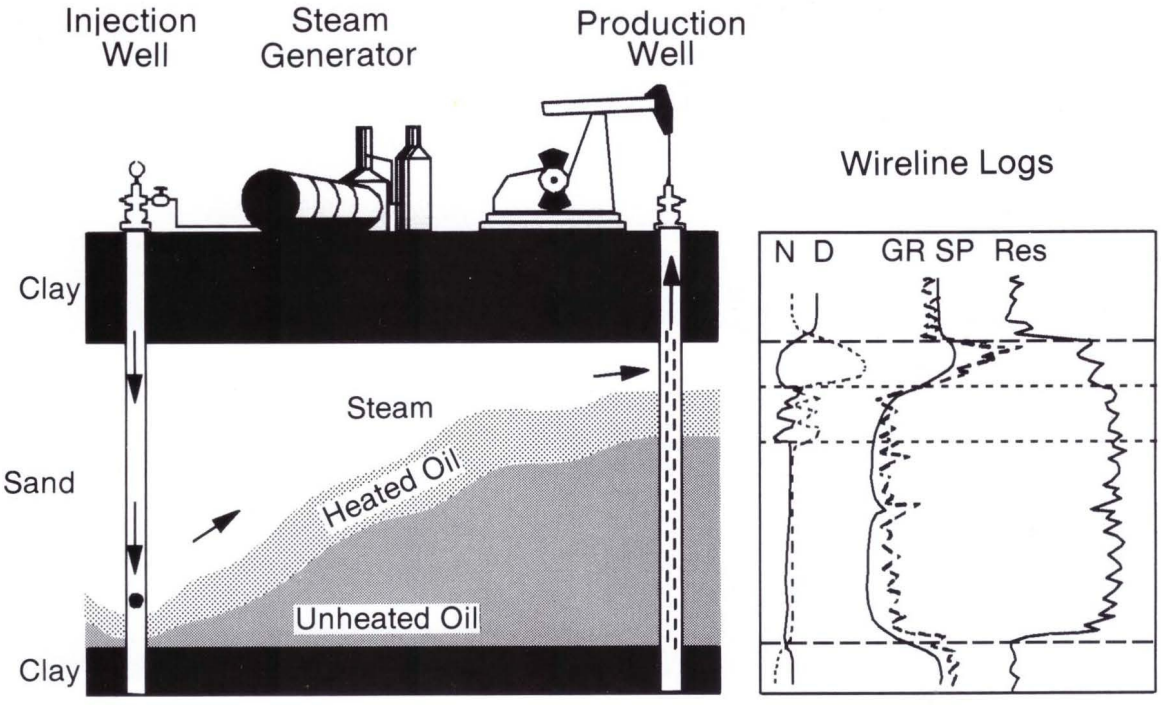

Fig. 5-19. Steamflood schematic showing an injection well and production well profile. Steam injected through a single (limited-entry) perforation near the base of a sand heats the oil which buoyantly rises to the top of the reservoir sand unit. Sand thickness typically ranges from 5 to 20 feet (1.5–6.1 m). Typical wireline log responses include a gas effect on neutron and density logs, a uranium roll-front on the gamma-ray log, and reversed SP signature in steamed intervals. (N = neutron porosity; D = density porosity; GR = gamma ray; SP = spontaneous potential; and Res = resistivity curve.)

geometries in the upper zones. These predictable characteristics, based on the depositional model, are verified by producing characteristics.

Generally the lower Tulare reservoir zones (D and E) are continuous and highly layered, because they represent delta-front sheet sands. Occasional thicker bedded mouth-bar sands link the thinner bedded and highly stratified distal-bar sands and serve as permeability conduits.

By contrast, the upper Tulare sands (zones A, B, and C) are channelized fluvial sequences that display considerable differences in flow-unit scale and form, reflecting the differences in character of the fluvial system from which they were deposited. The zone A and C sands are typical fine-grained meander-belt sands in that they are sinuous, elongate, and narrow (shoestring) bodies encased in mud (Fig. 5-8). Vertical and lateral communication between these sands is poor because of their limited interconnectedness. Accordingly, lateral flow-unit geometry is restricted. The zone B sands, representing coarse-grained meander-belt and braided fluvial systems, are commonly stacked and amalgamated to the extent that they perform as one highly connected reservoir (Fig. 5-8). Stacked channel sequences containing more than 75% sand can act effectively as a single [flow] unit due to their connectedness (Allen, 1978). However, with frontal displacement of oil during enhanced recovery processes, the scale of geologic heterogeneities relative to well spacing distinguishes baffles from barriers. Thin muds separating these sands are discontinuous over distances of tens of feet (meters) and are not effective barriers to steam with the existing well density, although they serve to baffle vertical flow. However, mud horizons which split the reservoir into layers over an area of several wells require both injection and production on both sides of that heterogeneity.

The effective reservoir-scale permeabilities throughout the Tulare are lower than measured core values by more than two orders of magnitude due to reservoir heterogeneities; effective reservoir permeability values used to simulate reservoir production behavior are as low as 1% of the measured core

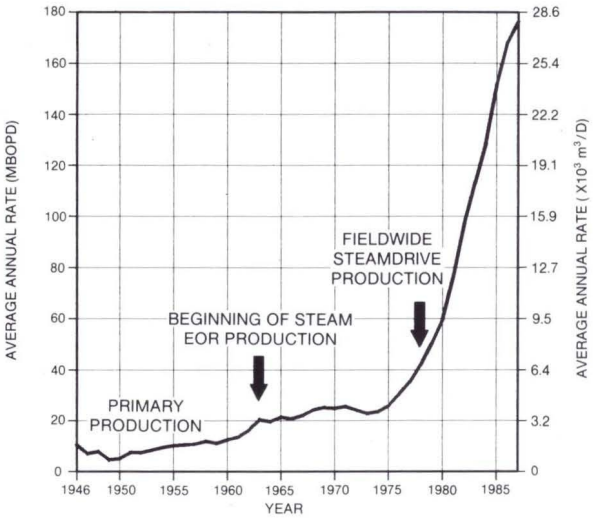

Fig. 5-20. Production history of the South Belridge Field. Up to 25% of this production is from non-Tulare reservoirs.

values (Dietrich, 1988). Both vertical and horizontal permeabilities are affected considerably by discontinuous clay interbeds which act as baffles or local barriers to vertical flow. As a consequence, effective reservoir-scale vertical permeability is calculated by the stochastic method of Begg and others (1985). Lateral permeability estimates are similarly decreased by the tortuosity created as a product of the amalgamation of sand bodies.

Production Characteristics

Well and Reservoir Performance

The Tulare reservoir at South Belridge Field has been produced by primary production, cyclic steaming, in situ combustion, and steamflood. Current production operations focus on steamflood development to produce the heavy (13–15° API gravity) oil (Fig. 5-20). Data presented here are mostly from the Mobil Oil Corporation-operated southern portion of the field, reflecting the authors' primary area of interest and data availability.

Primary field development wells were drilled on 10-acre (4.1-ha.) spacing, a distance between wells of 660 feet (201 m). These wells initially produced between 20 and 200 BOPD (3.2–32 m^3/D) and generally experienced a rapid decline. Wells typically produced 50 to 150 MBO (0.8–2.4 $\times$ 10^4 m^3) cumulative with 90% of the production occurring over a 20-year life. The primary producing mechanism was solution-gas drive with some assistance from gravity drainage and aquifer support on the flanks of the field. Initial reservoir pressure was probably hydrostatic at approximately 400 psi (2.8 $\times$ 10^3 kPa).

The first South Belridge Field thermal recovery pilot was an in situ combustion thermal-recovery (fireflood) experiment conducted from 1955 to 1958 (Gates and Ramey, 1958; Gates et al., 1978). This pilot demonstrated that viscous oil could be readily moved and oil recovery increased to 40 to 60% compared with a primary recovery of approximately 10%.

Cyclic steaming ("huff-n-puff") was started in 1963 and a fieldwide continuous steam injection line- drive operation began in 1969 (Fig. 5-20). The steamflood project was converted to 10-acre (4.1-ha.), inverted nine-spot steam patterns in the mid-1970s. Steam injectors are located at the center of a pattern with eight surrounding producing wells. This pattern configuration contains one injection well and three net producing wells, when patterns are developed side by side. With this arrangement, a well typically produces more than 200 MBO cumulative (3.2 $\times$ 10^4 m^3) of oil.

Existing steamflood patterns at South Belridge Field range from 2.5 to 10 acres (1.0–4.1 ha.) in size and each contains four to eight producing wells. Limited-entry perforations (Small, 1986) control the vertical steam injection profile in each cased injection well. This method can minimize the effects of lithofacies-controlled permeability variations at the well. Producing wells have traditionally used open-hole gravel-flow-pack, slotted liners, or wire-wrapped liners to provide sand control. Inside-casing gravel-packs have also been used to avoid completion in intermediate water sands or to avoid steam-desaturated reservoir sands.

Fluid properties in the Tulare change dramatically with the introduction of steam to the reservoir during steamflood. Oil saturations at South Belridge Field attain residual saturations commonly less than 5% and as low as 0% in steam-swept reservoir intervals. This is similar to other reported steamflood projects (Ali, 1982; Traverse et al., 1983). Due to density contrasts (gravity override), the steam rises to the top of reservoir flow units, commonly resulting in the lowest residual oil in the upper portions of the reservoirs (Ali and Meldau, 1979) (Fig. 5-19). Oil saturations below these swept zones are typically greater than 40%, and essentially original saturations occur at the base. Vertical and lateral distribution of reser-

voir lithofacies, structural dip, gravity override of steam, and seal continuity and thickness are natural factors influencing steam pathways.

Lithofacies-Related Considerations

The reservoir model of the Tulare at South Belridge Field shows strong dependence on depositional controls. This is evident at both the sand-body geometry scale and the smaller pore-throat scale. From an understanding of the depositional system, the reservoir model allows the prediction of reservoir geometry and quality and oil trapping potential. Permeability and oil saturation in the Tulare are directly related to depositional lithofacies, whereas the reservoir flow-unit geometries are dictated by the depositional system. Understanding the reservoir's three-dimensional geometry and flow-path continuity between wells is important for selecting completion intervals and well spacing, which are paramount to a successful steamflood.

The major differences in the reservoirs of the upper and lower Tulare can be explained by lithofacies types and their distribution. The upper Tulare fluvial-channel sands display the highest permeabilities and oil saturations, primarily reflecting their coarser grain sizes (Fig. 5-4). These channel sands have appreciably higher permeabilities than their associated finer-grained crevasse-splay and levee sands. The lower Tulare deltaic sands generally have lower than average permeabilities due primarily to their finer grain sizes and a small matrix-clay content.

Exploration And Production Strategy

Opportunities to discover another South Belridge Field are very limited. There are probably few onshore structures the size of the South Belridge anticline that have not been tested. The days of discovering major fields by surface expressions of anticlines with oil seeps in creek beds, as was the case for South Belridge, are long gone. However, existing fields with similar economic development potential to South Belridge have undoubtedly been overlooked.

The fundamental criterion for developing another South Belridge Field is to realize the extraordinary development potential of shallow, heavy-oil reservoirs, even when the discovery well is a poor producer. Isolated reservoir sand bodies in the initial wells may provide only a hint of the development potential in a fluviodeltaic reservoir complex. A critical early step is to look carefully at the geologic scale of potential reservoir units. Isolated well performance provides little indication of infill potential due to the highly variable scale of reservoir flow-unit geometries. During project planning, primary field development, and subsequent EOR operations, aspects of well spacing, pattern size and geometry, injection schedule, and completion plans can be matched with sand continuity models to make optimal use of EOR techniques.

Summary

The unconsolidated reservoir sands of the Pleistocene Tulare Formation at South Belridge Field contain heavy oil that is produced by more than 6,000 wells from depths generally less than 1,000 feet (305 m). Numerous stratigraphically discontinuous reservoir sands were deposited in a prograding fluviodeltaic depositional environment. The overall reservoir sequence contains laterally continuous reservoir sands in the lower zones and both coalescing and isolated "shoestring" geometries in the upper zones. Syndepositional structural growth of the anticline altered fieldwide distribution of sands. The reservoir model can predict the range of reservoir geometries and connectivity of the various reservoir horizons between wells.

Depositional lithofacies directly control reservoir properties due to the absence of diagenetic modification. Permeability and oil saturation are directly related to lithofacies, whereas the reservoir sand-body and reservoir flow-unit geometries are dictated by the depositional system. Depositional geometries of sands and clays and the structural overprint of the South Belridge anticline control the numerous oil-water contacts.

Primary production, cyclic steaming, steamflood injection, and in situ combustion methods have been used during the life of the field. Current production comes primarily from steamflood development of the field. The high density of wells involved in steamflood production defines small-scale reservoir flow units which would be geologically isolated and nonproductive with more widely spaced wells.

Opportunities for economic development of similar reservoirs with poor primary production benefit from comprehensive reservoir characterization and applications of new technology. These qualities are vital to engineering studies necessary to exploit the full potential of the field.

Acknowledgments. The authors appreciate and acknowledge the history and producing information contributed by E. Forrester, Jr. and mineralogical work performed by J.D. Cocker. We are grateful to M.G. Acosta, D.S. Anderson, J.M. Eagan, I.A. Fischer, R.J. Pashuck, and B.J. Welton for discussion and manuscript review. The manuscript benefited from review by T.H. Nilsen, G.F. Canjar, and the editors of this volume. Special thanks are due H.H. Mottern and Mobil Oil Corporation for sponsoring this work. Thanks to Mobil Oil Corporation and Mobil Research and Development Corporation for permission to publish this work.

Reservoir Summary

Field: South Belridge
Location: San Joaquin Valley, central California
Operators: Shell, Mobil, Exxon, Santa Fe Energy, Unocal, Mission Resources, and others
Discovery: 1911
Basin: San Joaquin basin
Tectonic/Regional Paleosetting: Wrench-faulted basin margin
Geologic Structure: Plunging anticline.
Trap Type: Stratigraphic pinch-out on a plunging anticline
Reservoir Drive Mechanism: Solution-gas drive with limited gravity drainage and aquifer support (primary)
- **Original Reservoir Pressure:** 400 psi (2.8×10^3 kPa) (assumed hydrostatic)

Reservoir Rocks:
- **Age:** Pleistocene
- **Stratigraphic Unit:** Tulare Formation
- **Lithology:** Gravel to very fine-grained sand; lithic feldsarenite
- **Depositional Environment:** Fluviodeltaic
- **Productive Facies:** Braided/meandering fluvial, distributary-channel, and distributary-mouth-bar sands
- **Petrophysics**
  - **ϕ:** Average 35%, range 32 to 42%; all primary intergranular (cores)
  - **k:** Average 3,000 md (air 300 psi [2.1×10^3 kPa]), range 100 to 10,000 md (cores)
  - **S_w:** Average 24%, range 15 to 90% (cores, logs)
  - **S_o:** 76% (cores)

Reservoir Dimensions
- **Depth:** 500 feet (152 m)
- **Areal Dimensions:** 2 by 10 miles (3.2×16 km)
- **Productive Area:** 8,700 acres (3,525 ha.)
- **Number of Reservoirs:** Multiple; 5 zones with 1 to 5 sands per zone
- **Hydrocarbon Column Height:** 900 feet (275 m)
- **Fluid Contacts:** Multiple oil-water contacts
- **Number of Pay Zones:** 5 to 7
- **Gross Sandstone Thickness:** 400 to 750 feet (122–229 m)
- **Net Sandstone Thickness:** 50 to 275 feet (15–84 m)
- **Net/Gross:** 0.3 to 0.7

Source Rocks
- **Lithology & Stratigraphic Unit:** Siliceous shale, Miocene Monterey Formation
- **Time of Hydrocarbon Maturation:** Late Miocene to Recent
- **Time of Trap Formation:** Pleistocene to Recent
- **Time of Migration:** Pleistocene to Recent

Hydrocarbons
- **Type:** Oil
- **GOR:** 45:1 SCF/bbl
- **API Gravity:** 13 to 14°
- **FVF:** 1.03
- **Viscosity:** 1,800 cP at 90°F (32°C); 7.9 cP at 300°F (149°C)

Volumetrics

- **In-Place:** N/A
- **Cumulative Production:** 700 MMBO (1.1×10^8 m³)
- **Ultimate Recovery:** 1,200 MMBO (1.9×10^8 m³) (estimated)
- **Recovery Efficiency:** N/A

Wells

- **Spacing:** 200 to 500 feet (61–152 m); 10 acres (4.1 ha.) primary, 2.5 to 10 acres (1.0–4.1 ha.) EOR patterns
- **Total:** 6,100 (currently active)
- **Dry Holes:** Less than 1%

Typical Well Production

- **Average Daily:** Primary 40 BO (6.4 m³); Steam EOR 80 BO (12.7 m³)
- **Cumulative:** Primary 50 to 100 MBO ($0.8–1.6 \times 10^4$ m³); Steam EOR 200 MBO (3.2×10^4 m³)

References

Ali, F.A., 1982, Steam injection theories—A unified approach: Society of Petroleum Engineers, Paper 10746, p. 309–315.

Ali, F.A., and Meldau, R.F., 1979, Current steamflood technology: Journal of Petroleum Technology, October, p. 1332–1341.

Allen, J.R.L., 1978, Studies in fluviatile sedimentation: An exploratory quantitative model for the architecture of avulsion-controlled alluvial suites: Sedimentary Geology, v. 21, p. 129–147.

Atwater, T., 1970, Implications of plate tectonics for the Cenozoic tectonic evolution of western North America: Geological Society of America Bulletin, v. 97, p. 97–109.

Barbat, W.F., and Galloway, J., 1934, San Joaquin Clay, California: American Association of Petroleum Geologists Bulletin, v. 18, p. 476–499.

Bartow, J.A., 1987, The Cenozoic evolution of the San Joaquin valley, California: U.S. Geological Survey Open-File Report 87-581, 74 p.

Beard, D.C., and Weyl, P.K., 1973, Influence of texture on porosity and permeability of unconsolidated sand: American Association of Petroleum Geologists Bulletin, v. 57, p. 349–369.

Begg, S.H., Chang, D.M., and Haldorsen, H.H., 1985, A simple statistical technique for calculating the effective vertical permeability of a reservoir region containing discontinuous shales, *in* Proceedings, 60th Annual Meeting of the Society of Petroleum Engineers, Paper 14271, 15 p.

California Division of Oil and Gas, Department of Natural Resources, 1950, 36th Annual Report State Oil and Gas Supervisor 1950: v. 36, p. 18–25.

California Division of Oil and Gas, Department of Conservation, 1985, California Oil and Gas Fields, Central California, Vol. I.

California Division of Oil and Gas, Department of Conservation, 1987, 72nd Annual Report of the State Oil and Gas Supervisor 1986: v. 72, p. 57–58.

Clarke S.H., Jr., Howell, D.G., and Nilsen, T.H., 1975, Paleogene geography of California, *in* Weaver, D.W., Hornaday, G.R., and Tipton, A., eds., Paleogene Symposium and Selected Technical Papers: Long Beach, California, American Association of Petroleum Geologists—Society of Economic Paleontologists and Mineralogists—Society of Exploration Geophysicists, Pacific Sections, p. 121–154.

Connan, J., and Coustau, H., 1987, Influence of the geological and geochemical characteristics of heavy oil on their recovery, *in* Meyer, R. F., ed., Exploration for Heavy Crude Oil and Natural Bitumen: American Association of Petroleum Geologists Studies in Geology 25, p. 261–279.

Dickinson, W.R., Ingersoll, R.V., and Graham, S.A., 1979, Paleogene sediment dispersal and paleotectonics in northern California: Geological Society of America Bulletin, v. 90, Pt I, p. 898–899, Pt II, p. 1458–1528.

Dietrich, J., 1988, Steamflooding in a waterdrive reservoir: Upper Tulare sands, South Belridge field, *in* Proceedings, 1988 California Regional Meeting: Society of Petroleum Engineers, Paper 17453, p. 479–494.

Elkins, L.F., 1972, Uncertainty of oil in place in unconsolidated sand reservoirs—A case history: Journal of Petroleum Technology, November, p. 1315–1319.

Ethridge, F.G., and Schumm, S.A., 1978, Reconstructing paleochannel morphologies and flow characteristics: Methodology, limitations, and assessment, *in* Miall, A.D., ed., Fluvial Sedimentology: Canadian Society of Petroleum Geologists Memoir 5, p. 703–721.

Fielding, C.R., and Crane, R.C., 1987, An application of statistical modelling to the prediction of hydrocarbon recovery factors in fluvial reservoir sequences, *in* Ethridge, F. G., Flores, R. M., and Harvey, M. D., eds., Recent developments in fluvial sedimentology: Society of Economic Paleontologists and Mineralogists Special Publication 39, p. 321–327.

Folk, R.L., Andrews, P.B., and Lewis, D.W., 1970, Detrital sedimentary rock classification and nomenclature for use in New Zealand: New Zealand Journal of Geology and Geophysics, v. 13, p. 937–968.

Foss, C.D., 1972, A note on the fluid level traps in the San

Joaquin valley, *in* Rennie, E.W., Jr., ed., Geology and Oil Fields, West Side Central San Joaquin Valley: American Association of Petroleum Geologists Pacific Section, Guidebook, p. 15.

Gates, C.F., and Brewer, S.W., 1975, Steam injection into the D&E zones, Tulare Formation, South Belridge field, Kern County, California: Journal of Petroleum Technology, v. 27, p. 343–348.

Gates, C.F., and Ramey H.J., Jr., 1958, Field results of South Belridge thermal recovery experiment: American Institute of Mining, Metallurgical, and Petroleum Engineering Petroleum Transactions, v. 213, p. 236–244.

Gates, C.F., Jung, K.D., and Surface, R.A., 1978, In-situ combustion in the Tulare Formation, South Belridge Field, Kern County, California: Journal of Petroleum Technology, v. 30, p. 798–806.

Graham, S.A., 1987, Tectonic controls on petroleum occurrence in California, *in* Ingersoll, R.V. and Ernst, W.G., eds., The Geotectonic Development of California, Rubey Volume VI: Englewood Cliffs, New Jersey, Prentice-Hall, p. 47–63.

Graham, S.A., and Williams, L.A., 1985, Tectonic, depositional, and diagenetic history of Monterey Formation (Miocene), central San Joaquin basin, California: American Association of Petroleum Geologists Bulletin, v. 69, p. 385–411.

Harding, T.P., 1976, Tectonic significance and hydrocarbon trapping consequences of sequential folding synchronous with San Andreas faulting, San Joaquin valley, California: American Association of Petroleum Geologists Bulletin, v. 60, p. 356–378.

Ingersoll, R.V., 1979, Evolution of the Late Cretaceous forearc basin, northern and central California: Geological Society of America Bulletin, v. 90, p. 813–826.

Lennon, R.B., 1976, Geological factors in steam-soak projects on the west side of the San Joaquin basin: Journal of Petroleum Technology, v. 4, p. 741–748.

Lettis, W.R., 1982, Late Cenozoic stratigraphy and structure of the western margin of the central San Joaquin valley, California: U.S. Geological Survey Open-File Report 82-526, 26 p.

McPherson, J.G., Shanmugam, G., and Moiola, R.J., 1987, Fan-deltas and braid deltas: Varieties of coarse-grained deltas: Geological Society of America Bulletin, v. 99, p. 331–340.

Namson, J.S., and Davis, T.L., 1988, Seismically active fold and thrust belt in the San Joaquin valley, central California: Geological Society of America Bulletin, v. 100, p. 257–273.

Nilsen, T.H., and Clarke, S.H., Jr., 1975, Sedimentation and tectonics in the early Tertiary continental borderland of central California: U.S. Geological Survey Professional Paper 925, 64 p.

Oil and Gas Journal, 1988, Forecast and Review, v. 86, p. 60.

Sedimentology Research Group, 1981, The effects of in-situ steam injection on Cold Lake oil sands: Bulletin of Canadian Petroleum Geology, v. 29, p. 447–478.

Small, G.P., 1986, Steam-injection profile control using limited-entry perforations: Society of Petroleum Engineers Production Engineering, September, p. 388–394.

Stanton, R.J., and Dodd, J.R., 1970, Paleoecologic techniques—Comparison of faunal and geochemical analyses of Pliocene paleo-environments, Kettleman Hills, California: Journal of Paleontology, v. 44, p. 1092–1121.

Traverse, E.F., Deibert, A.D., and Sustek, A.J., 1983, San Ardo—A case history of a successful steamflood: Society of Petroleum Engineers, Paper 11737, 8 p.

Webb, G.W., 1981, Stevens and earlier Miocene turbidite sandstones, southern San Joaquin valley, California: American Association of Petroleum Geologists Bulletin, v. 65, p. 438–465.

Woodring, W.P., Steward, R., and Richards, R.W., 1940, Geology of the Kettleman Hills Oilfield, California: U.S. Geological Survey Professional Paper 195, 170 p.

Key Words

South Belridge Field, California, San Joaquin basin, Tulare Formation, Pleistocene, fluviodeltaic, distal bar, mouth bar, meandering fluvial, braided fluvial, heavy oil, steamflood, enhanced oil recovery, in situ combustion, San Andreas fault, petrophysics, reservoir heterogeneity.